KEY CONTROL TECHNOLOGIES OF STATCOM-APF-LCL COMPOSITE COMPENSATION DEVICE UNDER REMOTE TELEMETRY

Haiyan Liu[1], Jianzhen Liu[1,], Jianglong Li[1], Guannan Li[1], Zhiqin Wen[1]*
[1]State Grid Shanxi Electric Power Company Lvliang Power Supply Company, Shanxi, Lvliang 03300, China

Abstract - To address reactive power fluctuations and harmonic pollution in renewable energy grid integration, a novel composite compensation device combining a remotely controllable Static Synchronous Compensator and an Active Power Filter based on Inductor–Capacitor–Inductor topology is developed. The hierarchical decision-making mechanism based on expert systems and the fuzzy-PI dual-loop control strategy were applied to the system, enabling rapid reactive power regulation and wide-frequency harmonic suppression. Research conducted under typical irradiance fluctuation conditions involved Matlab/Simulink simulations, analyzing the system's performance in terms of DC bus voltage stability, grid current quality, and reactive power regulation. Further simulations demonstrated that 5G networks outperformed traditional LANs in communication latency and reliability, enhancing control response speed and system stability. Additionally, preliminary energy consumption and operational cost analysis indicated that this composite compensation system possessed certain economic advantages. This study provides theoretical support and methodological reference for engineering applications of high-performance, multifunctional grid compensation systems under renewable energy integration conditions

Keywords: Reactive power compensation; Harmonic mitigation; Static Synchronous Compensator; Active Power Filter; Fuzzy control.

1. Introduction

In recent years, the rapid development of distributed photovoltaic (PV) power generation has imposed higher demands on the operational stability of distribution networks. Since the output power of PV systems is highly sensitive to variations in solar irradiance and temperature, this leads to bus voltage fluctuations and power imbalance [1–3]. Meanwhile, with the widespread use of power electronic equipment and nonlinear loads on the end-user side, the harmonic content in distribution networks has significantly increased, adversely affecting power quality and equipment safety [4–6]. Although conventional Static Var Compensators (SVCs) and shunt Active Power Filters (APFs) can partially mitigate these issues. But they exhibit notable limitations in terms of dynamic response speed, adaptive capability, and system compatibility; this makes them insufficient for meeting the real-time regulation requirements under high-penetration distributed energy scenarios.

The emergence of hybrid compensation technology provides a new solution to these challenges. A novel compensation device that can mitigate harmonics and compensate reactive power at the same time can remarkably improve the operation quality of distribution systems by integrating active filtering and reactive power regulation technology [7,8]. On this basis, combined with modern communication and intelligent control technology, the collaborative and intelligent development of remote compensation system is further promoted. Real-time data interaction and distributed control enabled by Fifth Generation Mobile Communication (5G) and edge computing platforms help overcome the communication bottlenecks and response delays inherent in traditional centralized control; thereby, it improves overall control flexibility and operational efficiency [9–11]. Multi-level control methods incorporating artificial intelligence-based decision-making mechanisms have become a research focus in power compensation strategies; this demonstrates strong adaptability and robustness in identifying

dx.doi.org/10.17683/ijomam/issue23.3

complex operating conditions and optimizing compensation strategies [12].

This study handles power quality issues in distribution networks with PV distributed generation by designing a hybrid compensation device with remote coordination capabilities. This device functionally coordinates and structurally integrates the Static Synchronous Compensator (STATCOM) and the APF based on the Inductor–Capacitor–Inductor (LCL) topology; this achieves unified control of reactive power regulation and harmonic suppression. When it comes to control architecture, this study introduces 5G communication and edge computing platforms and creates a hierarchical distributed control system for remote scenarios. The study also compares how communication delays affect performance control by using delay modelling. The control strategy uses an expert system and fuzzy control mechanisms; it can adjust the dual closed-loop Proportional-Integral (PI) control parameters online. This makes the system respond better to sudden changes in light and disturbances in the load. Unlike previous studies that simply use STATCOM or APF for local compensation or rely solely on traditional PI control strategies, the innovation of this study lies in: (1) Integrating the functions and structures of STATCOM and LCL-APF composite structures to achieve coordinated compensation of reactive power and harmonics; (2) Introducing 5G communication and edge computing, taking the communication network as an active control factor, building a hierarchical distributed control architecture, and supporting remote collaborative control; (3) Integrating expert systems with fuzzy PI control to achieve online adaptive tuning of PI parameters, enabling the system to have stronger robustness under dynamic disturbances and parameter fluctuations. Through these comprehensive designs, the proposed method expands the application scenarios of composite compensation devices, and differs from existing solutions in control strategies and remote communication integration. This forms a systematic solution that can improve power quality under high proportion photovoltaic access conditions. In order to clearly demonstrate the overall technical route and methodological process of this study, Figure 1 presents a schematic diagram of the complete research process from problem analysis to conclusion verification.

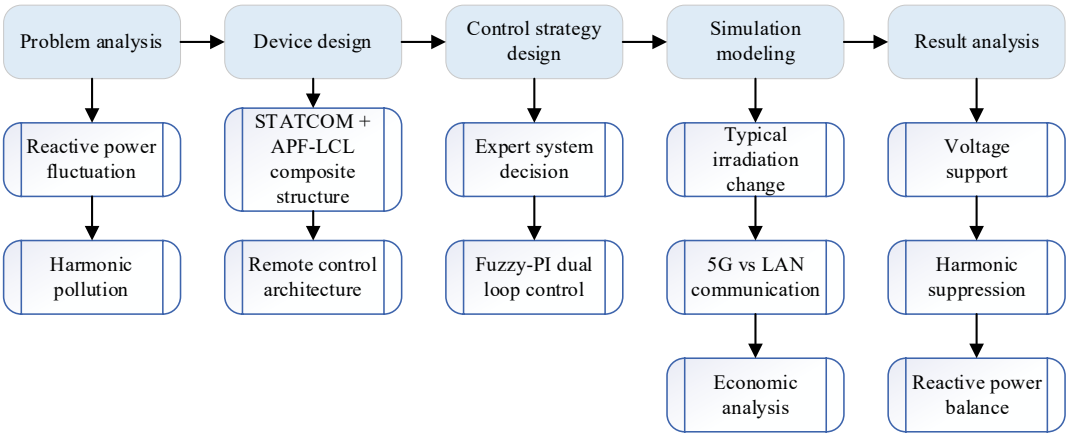

Figure 1: Technical route and process diagram

2. Related Work

With the continuous expansion of PV power generation, the resulting power quality issues in distribution networks have increasingly become critical factors constraining the stable operation of such systems. In the field of power quality control for PV-integrated distribution networks, Guo and Xu proposed a harmonic suppression and reactive power compensation strategy based on multifunctional grid-connected PV inverters, along with a three-level optimization model utilizing an adaptive ant colony algorithm to optimize the power quality of grid-connected PV systems [13]. Bajaj and Singh developed a global power quality index based on the analytic hierarchy process to simplify power quality assessment in renewable energy-based distributed generation systems. By integrating the power quality indicators of various bus groups, the method provided a comprehensive assessment tool for utilities, loads, and the overall system [14]. Boopathi and Indragandhi designed a novel predictive direct power control strategy for a parallel APF model based on a three-level neutral-point-clamped inverter. The approach aimed to reduce harmonics caused by nonlinear loads and address reactive power issues in distribution systems [15].

In terms of control strategies for compensation devices, Kumar et al. integrated a battery energy storage system with a distributed SVC based on fuzzy logic control to enhance the response capability of hybrid energy systems under low-voltage ride-through scenarios.

Thus, they improved voltage quality at both the direct current (DC) link and the point of common coupling [16]. Zheng and Wei investigated assist current control in electric power steering systems. Their method effectively reduced steady-state error and improved adaptability during steering maneuvers by dynamically adjusting the PI control parameters using fuzzy rules; this could enhance handling stability under extreme conditions [17]. Cheng et al. proposed a novel two-level coordinated voltage control strategy that combined regional and global control to address voltage security issues caused by power imbalances between distributed PV generation and loads in active distribution networks [18].

Although existing studies have made certain progress in harmonic suppression and reactive power compensation, most focus on a single compensation approach and lack composite strategies that simultaneously address harmonic mitigation and reactive power fluctuation control. There is still a contradiction between the complexity of control structure and real-time performance. In addition, under the dynamic disturbance, some control methods have the problems of response delay or insufficient steady-state accuracy; this makes them unsuitable for the frequent fluctuation characteristics of PV systems. In respond to these challenges, this study puts forward a STATCOM+APF-LCL composite compensation scheme based on an expert system and fuzzy-PI dual-loop control. The scheme balances multifunctional performance and fast dynamic response; meanwhile it is verified by simulation in bus voltage support, reactive power stability and broadband harmonic suppression.

3. Design and Control Strategy of the Compensation Device

3.1 Overall Structural Design of the Compensation Device

The primary power quality issues in PV grid-connected systems include harmonic pollution and reactive power fluctuations [19,20]. In order to effectively enhance power quality, a composite compensation system integrating an Active Power Filter with an Inductor–Capacitor–Inductor structure (APF-LCL) and a STATCOM is designed. This system connects in parallel with the power grid, offering both filtering and reactive power support capabilities, thereby improving voltage quality and system stability. The whole structure adopts two-layer compensation structure: the upper layer is composed of APF based on LCL filter, and the lower layer is deployed with low-capacity STATCOM. APF adopts hysteresis current tracking control strategy, while STATCOM uses fuzzy PI double-loop control mechanism to realize fast response and dynamic compensation. Key system components include three-phase bridge-type voltage source converter (VSC), LCL filter unit, energy storage capacitor, shunt transformer, system coupling inductor and harmonic current tracking unit for real-time detection and control. The comprehensive structure is shown in Figure 2.

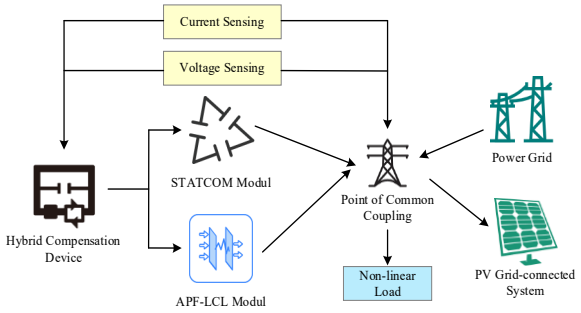

Figure 2: Overall structure of the APF-LCL + STATCOM hybrid compensation device

(1) APF-LCL subsystem topology structure

APF-LCL is a typical LCL filter composed of an inverter side inductor L_1, a parallel capacitor C, and a grid side inductor L_2 connected in series. The circuit diagram is shown in Figure 3.

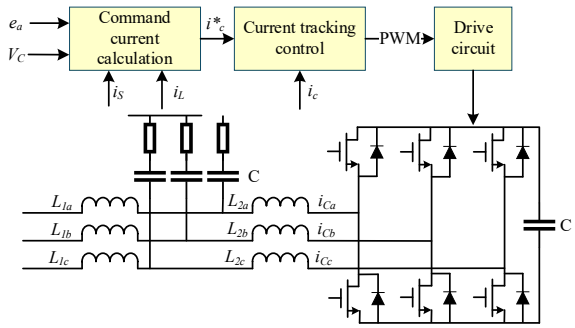

Figure 3: APF-LCL circuit structure diagram

The output voltage $u_a(t)$ of the inverter is applied to the parallel capacitor through L_1, and the capacitor voltage $u_c(t)$ is then transmitted to the grid voltage $e_a(t)$ through the grid side inductor, forming a third-order filtering network. The current sampling point is set on the grid side, which facilitates the APF to construct real-time command current based on the grid side harmonic current, and uses hysteresis current control to achieve fast dynamic tracking and harmonic compensation. The dynamic characteristics of LCL filters can be described by the following system of differential equations:

$$L_1 \frac{di_1(t)}{dt} + R_1 i_1(t) = u_a(t) - u_c(t) \quad (1)$$

$$u_c(t) = (i_1(t) - i_2(t))(R_d + \frac{1}{j\omega C}) \quad (2)$$

$$L_2\frac{di_2(t)}{dt} + R_2 i_2(t) = u_c(t) - e_a(t) \quad (3)$$

R_1 and R_2 represent the stray resistance of the corresponding circuit, L_1, C, L_2 describe the dynamic behavior of the inverter side inductance, capacitor branch, and grid side inductance, respectively, while $i_1(t)$, $i_2(t)$, $u_c(t)$, correspond to the current/voltage paths labeled in Figure 2. Transforming the equations above into the Laplace domain and combining them yields:

$$\begin{bmatrix} U_a(s) \\ E_a(s) \end{bmatrix} = \begin{bmatrix} L_1 s + R_1 & 0 \\ 0 & L_2 s + R_2 \end{bmatrix} \begin{bmatrix} I_1(s) \\ I_2(s) \end{bmatrix} + \begin{bmatrix} 1 \\ -1 \end{bmatrix} U_c(s) \quad (4)$$

By constructing a reference current $i_c^*(t)$, the actual compensation current $i_c(t)$ is dynamically tracked using hysteresis current control, ensuring that the APF compensates for low-frequency harmonics not filtered by the LCL structure in real time. The core principle of hysteresis control is to compare the deviation between the actual and reference currents:

$$\Delta i_c(t) = i_c^*(t) - i_c(t) \quad (5)$$

Based on whether this deviation falls within a predefined hysteresis bandwidth, the system triggers the pulse-width modulation (PWM) modulator to output switching control signals.

(2) STATCOM subsystem topology structure

The lower compensation module is a small capacity STATCOM, and the circuit structure is shown in Figure 4.

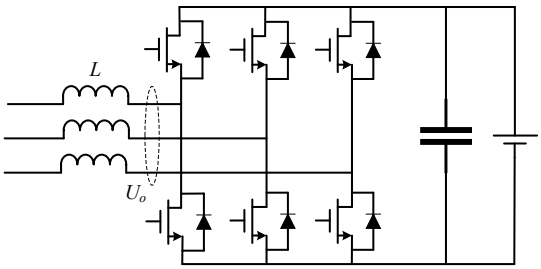

Figure 4: STATCOM circuit structure diagram

For reactive power compensation, the STATCOM adjusts the amplitude and phase of the VSC output voltage to absorb or inject reactive power. Its equivalent circuit is modeled as a voltage source in series with a system inductor. Let U_s denote the system voltage, U_o the STATCOM output voltage, and δ the phase angle between them; then, the active and reactive power expressions are:

$$Q = \frac{U_s U_o \sin(\delta)}{X} \quad (6)$$

$$P = \frac{U_s U_o \cos(\delta) - U_s^2}{X} \quad (7)$$

In this context, X is the equivalent reactance. According to the voltage vector control principle, when $\delta > 0$, the STATCOM injects capacitive reactive power; when $\delta < 0$, it absorbs inductive reactive power, thereby enabling dynamic voltage regulation and support.

APF-LCL and STATCOM operate in parallel throughout the entire system, with complementary functions and independent topologies but coupled control variables. APF-LCL is responsible for wideband harmonic control, making the grid side current approach the ideal sine waveform; STATCOM is responsible for dynamic reactive power support to reduce voltage fluctuations at the grid connection point; APF improves current quality, STATCOM improves voltage quality, and both work together to optimize the comprehensive power quality of the grid connection point.

3.3 Control System Architecture Design

To meet the stringent requirements for response speed, control precision, and communication reliability in PV grid-connected compensation systems, a hierarchical control system based on 5G and edge computing architecture is constructed. The system adopts a three-tier structure of central control center, edge control nodes and local execution units. It fuses centralized coordination, intelligent edge-level decision-making and high-speed local response ability; this can realize real-time control under dynamic load and PV power fluctuation. Figure 5 shows the overall control system architecture.

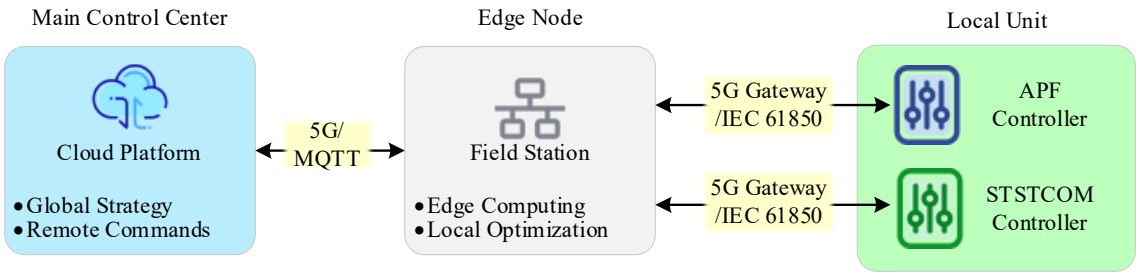

Figure 5: Remote control system architecture

The central control center is deployed on a cloud platform; it is responsible for tasks such as operational state monitoring, power balance assessment, global compensation strategy formulation and the issuance of remote control commands. This layer establishes high-speed, low-latency data channels with edge nodes via the 5G public network, supporting millisecond-level response and synchronized periodic task scheduling. Edge control nodes are installed at on-site control stations near the compensation equipment. They are equipped with edge computing chips and local data caching modules, capable of intelligently parsing and locally optimizing the strategies issued by the central controller. These nodes also monitor how the device is operating and the environmental conditions, filter data in real-time and respond to events, and carry out important control strategies locally. At the communication protocol level, the edge nodes and the central control center use a system called Message Queuing Telemetry Transport (MQTT) to share data efficiently. The local execution units include STATCOM and APF-LCL control modules; each module can run independently. These units connect directly to electrical systems and handle the final control signals. Both modules integrate fast PWM or Sinusoidal Pulse Width Modulation (SPWM) drive controller, real-time current/voltage sampling channel and feedback loop control algorithm to ensure control accuracy and dynamic response speed. The local layer establishes a real-time control link with the edge nodes through the 5G gateway; this supports the time synchronization under International Electrotechnical Commission 61850 (IEC 61850) standard.

This realizes millisecond-level state adjustment and coordinated action, and guarantees seamless cooperation among multiple compensation units. The central controller, edge nodes and local execution units form a closed-loop feedback system; this system balances global optimization and fast local response. The architecture supports the operation of various heterogeneous compensation devices while significantly improving the stability, scalability and fault tolerance of the system.

3.4 Integrated Control Strategy for the Hybrid Compensation Device

- ***Expert System-Based Decision Mechanism***

In PV grid-connected systems, the frequent change of reactive power demand caused by load fluctuation requires a reactive power compensation strategy; thus, it can be identified in real time and respond quickly to guarantee voltage stability and improve power quality. Considering the rising cost associated with high-capacity traditional SVCs, this system adopts decision-making mechanism based on expert system as its core. This approach realizes the coordinated operation of APF-LCL filter groups and a low-capacity STATCOM. Through intelligent evaluation of grid operating conditions at the strategy level, the system dynamically allocates compensation resources, thereby enhancing operational efficiency while considering cost control [21–23]. The structural schematic is shown in Figure 6.

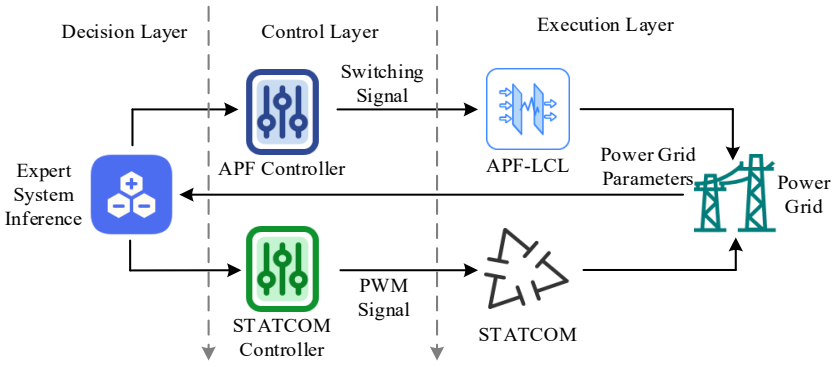

Figure 6: Structure of the expert decision system

The expert system adopts a three-layer architecture: execution, control and decision. The execution layer includes STATCOM and several APF-LCL units; they are responsible for performing compensation tasks. The control layer consists of independent PWM/SPWM pulse generation controllers; they are used to receive decisions and send corresponding control signals. As a core module, the decision layer embeds expert rule base and inference engine. It evaluates the grid's reactive power deficit based on real-time sampled data and determines the operating strategies for each compensation unit through rule-based reasoning.

The control strategy performs quantitative analysis based on the system's total reactive power demand and the real-time available compensation capacity. Assume the system is equipped with *n* APF-LCL units, each providing an equivalent capacitive reactive power compensation of Q_C, and that the STATCOM has a capacity of $2Q_C$. Given current operating conditions, the number of APF units to be activated, denoted by K, is calculated based on load

fluctuations. The system's compensation capability must then satisfy the following condition:

$$2(n-k+1)Q_C \le Q \le 2(n-k+2)Q_C \quad (8)$$

In Eq. (8), Q is the current reactive power deficit, and k is the number of APF units deactivated. Under this condition, the expert system determines the expected reactive power output of the STATCOM, Q_{ref}, as:

$$Q_{ref} = Q - (n-k)Q_C \quad (9)$$

This equation is used to control the amount of reactive power output by the STATCOM to compensate for the remaining deficit not covered by the activated APF units. Based on the real-time calculation results, the decision layer transmits Q_{ref} and K to the STATCOM and APF controllers; they then generate PWM control signals to execute the compensation actions.

The expert system fuses fuzzy logic with rule-based reasoning to guarantee fast response and redundant fault tolerance. When external interference causes frequent system state switching, the expert system can refer to historical data trends and current state to predict and adjust future decisions; this can avoid unstable power quality caused by excessive switching.

- ***Fuzzy-PI Dual-Loop Control Strategy***

In order to enhance the STATCOM's dynamic compensation performance and robustness, a fuzzy controller is introduced into the conventional dual-loop PI control structure; this forms a fuzzy-PI dual-loop coordinated control framework. This approach improves the system's adaptability to disturbances and parameter variations. The control system adopts a typical dual closed-loop structure composed of a DC-side voltage outer loop and an alternating current (AC)-side current inner loop. The fuzzy controller acts on the voltage outer loop to adjust PI parameters in real time. The system structure is illustrated in Figure 7.

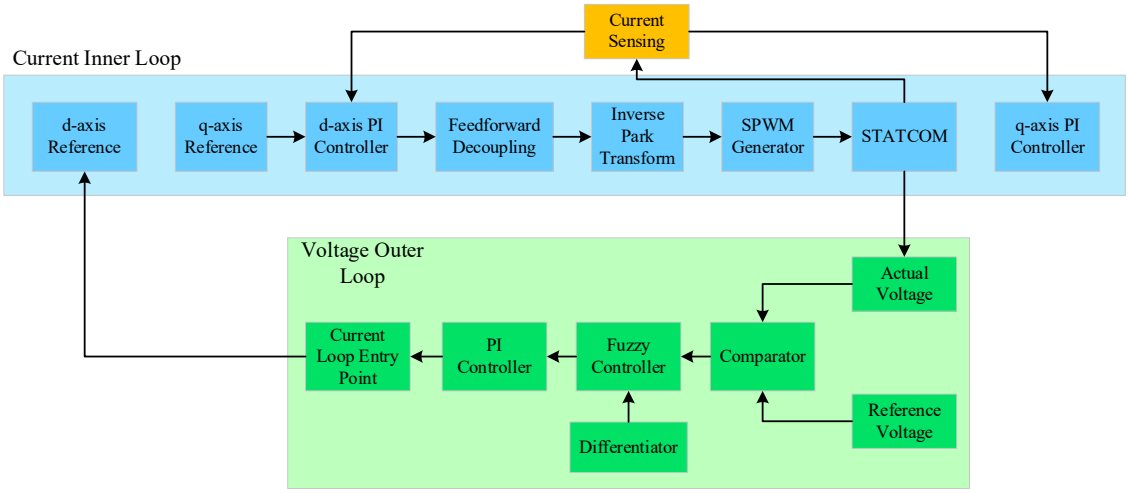

Figure 7: Structure of the fuzzy-PI dual-loop control system

In the outer loop, the error between the DC voltage v_{dc} and the reference value v_{dc}^* is defined as Eq. (10):

$$e(t) = v_{dc}^* - v_{dc}(t) \quad (10)$$

The rate of change of error is expressed as Eq. (11):

$$\Delta e(t) = \frac{de(t)}{dt} \quad (11)$$

To facilitate fuzzy inference operations, the error $e(t)$ and error change rate $\Delta e(t)$ are first normalized and mapped to the interval [-1,1]. Their scaling factors are selected according to the allowable fluctuation range of DC voltage and the dynamic characteristics of the system. The fuzzy controller takes $e(t)$ and $\Delta e(t)$ as input variables, and the proportional gain increment Δk_p and integral gain increment Δk_i as output variables. It realizes online adjustment of PI parameters through fuzzy inference. The outer-loop PI control law can be expressed as:

$$i_d^*(t) = k_p(t) \cdot e(t) + k_i(t) \int e(t)dt \quad (12)$$

$k_p(t) = k_{p0} + \Delta k_p$; $k_i(t) = k_{i0} + \Delta k_i$; k_{p0} and k_{i0} are the initial PI parameters. $i_d^*(t)$ represents the current command of STATCOM on the d-axis.

The input and output of the fuzzy controller are divided into seven levels of fuzzy variables: negative large, negative medium, negative small, zero, positive small, positive median, and positive large. The membership functions of all fuzzy variables adopt symmetric triangular functions; they are

evenly distributed within the input and output universes of discourse to ensure continuity and smoothness of the inference process. The fuzzy rule base is designed based on STATCOM voltage regulation experience and control objectives. When the voltage error is large and the error change rate increases in the same direction, the proportional gain is increased to accelerate dynamic response. When the error gradually decreases or the error change rate approaches zero, the proportional gain is appropriately reduced and the integral effect is increased to minimize steady-state error and suppress overshoot. For example, when both $e(t)$ and $\Delta e(t)$ are positive large, a large Δk_p and a medium Δk_i are selected. When $e(t)$ is negative small and $\Delta e(t)$ is zero, Δk_p is appropriately reduced and Δk_i is set to zero to enhance system stability. The entire fuzzy rule base contains 49 rules in total, covering all combinations of input variables. The fuzzy inference process adopts the max-min inference method, and the centroid method is used for defuzzification to obtain continuous Δk_p and Δk_i, thus achieving smooth online adjustment of PI parameters. In this way, the outer-loop control can adaptively adjust the control intensity under different light disturbances and load changes, improving the rapidity and stability of DC bus voltage regulation.

The current inner loop decouples the active and reactive components in the dq rotating reference frame. Its mathematical model is given by Eq. (13):

$$\begin{bmatrix} \frac{di_d}{dt} \\ \frac{di_q}{dt} \end{bmatrix} = \frac{1}{L}\begin{bmatrix} u_{sd} - u_d - Ri_d + \omega Li_q \\ u_{sq} - u_q - Ri_q - \omega Li_d \end{bmatrix} \tag{13}$$

To eliminate the current coupling term, a feedforward decoupling voltage is introduced, which is defined as:

$$\begin{cases} u_{d,ff} = u_{sd} - Ri_d + \omega Li_q \\ u_{q,ff} = u_{sq} - Ri_q - \omega Li_d \end{cases} \tag{14}$$

The dq axis PI controller outputs a regulation based on current error, and the control strategy expression is:

$$\begin{cases} u_{d,pi} = k_{pd}(i_d^* - i_d) + k_{id}\int(i_d^* - i_d)dt \\ u_{q,pi} = k_{pq}(i_q^* - i_q) + k_{iq}\int(i_q^* - i_q)dt \end{cases} \tag{15}$$

In Eq. (15), i_q^* is obtained from the reactive power detection module, typically estimated in real time using the p-q theory or the i_p-i_q method. These approaches extract the fundamental current components through coordinate transformation and filtering, thereby improving the accuracy of reactive current tracking.

The final control voltage is:

$$\begin{cases} u_d = u_{d,ff} + u_{d,pi} \\ u_q = u_{q,ff} + u_{q,pi} \end{cases} \tag{16}$$

Accurate tracking of STATCOM output current and fast dynamic reactive power compensation are realized by dq →αβ inverse transformation and SPWM modulator output drive signal.

The fuzzy-PI double-loop control strategy fuses the steady-state accuracy of traditional PI control with the adaptive ability of fuzzy logic; it also improves the dynamic response speed and robustness of the system to uncertain interference.

4. Results and Analysis

4.1 Simulation Modeling

In order to verify the reactive power regulation and harmonic mitigation performance of the STATCOM and APF-LCL composite compensation system under PV grid-connected conditions, an integrated simulation platform consisting of a PV module, STATCOM, and APF-LCL is developed. The system adopts a hierarchical control architecture combining an expert system and a fuzzy-PI controller. SPWM is used to achieve high-precision current tracking; this effectively reduces the delay issues associated with traditional harmonic detection methods.

The power output by PV module is boosted by Boost converter, stabilized by DC/DC converter, and then connected to DC bus. On the inverter side, the system is connected to the power grid through an LCL filter; this eliminates high-frequency harmonic residues. In contrast, APF provides real-time compensation. STATCOM is connected in parallel on the bus side to adjust the phase and amplitude of its output voltage to realize dynamic reactive power regulation and voltage support.

The system adopts 5G edge computing framework; the central control center, edge nodes and execution units realize multi-level control synchronization through MQTT protocol; this enhances real-time performance and system coordination. The control strategy uses the equivalent current detection method to generate the reference current; the fuzzy controller dynamically adjusts the PI parameters to balance the stability of the voltage outer loop and the fast response of the current inner loop. This design improves the robustness and dynamic adaptability of the whole system.

The simulation model is implemented in Matlab/Simulink. The operational parameters are listed in Table 1. The Matlab/Simulink simulation architecture is demonstrated in Figure 8.

Table 1: Simulation parameter settings

Parameter name	Value	Unit	Description
Voltage level	380	V	System phase voltage
Power grid capacity	1000	kVA	Grid-connected capacity
System frequency	50	Hz	Power frequency
Active power of parallel load	10	kW	Load active power
Reactive power of parallel load	10	kVar	Load reactive power
Grid-connected inductor	0.006	H	Grid-connected inductance
LCL filter inverter side inductance	0.002	H	APF-LCL inductance
LCL filter grid side inductance	0.002	H	APF-LCL inductance
LCL filter capacitor	0.22	F	APF-LCL filtering capacitor
LCL filter resistor	0.05	Ω	Inverter side stray resistance
LCL filter resistor	0.05	Ω	Network side stray resistance
STATCOM rated capacity	50	kVA	Capacity of parallel compensation device
STATCOM DC side reference voltage	800	V	DC bus voltage reference
Initial parameters k_p and k_i of PI controller	0.1/50	-	Initial values of inner loop PI parameters
Hysteresis bandwidth	2	A	APF current hysteresis bandwidth
Simulated lighting intensity	1000	W/m^2	Photovoltaic input conditions
Ambient temperature	25	°C	Photovoltaic environmental temperature

4.2 Simulation Results and Analysis of the Compensation Device and Control Strategy

In order to assess the voltage support and compensation performance of STATCOM+APF-LCL hybrid compensation system under fluctuating solar irradiance, a simulation scenario of step change of irradiance is designed. The system's voltage stability under disturbance and the proposed control strategy's effectiveness are evaluated by observing the response characteristics of DC bus voltage. Changes in PV output can cause fluctuations in DC bus voltage; this can have a negative effect on the output of the inverter and the quality of the electricity supplied to the grid. The control system quickly makes the STATCOM adjust the reactive power to stabilize the bus voltage. At the same time, the APF-LCL suppresses current harmonics caused by the disturbance. Figure 9 shows how changes in light intensity affect the DC bus voltage when the temperature is 25°C.

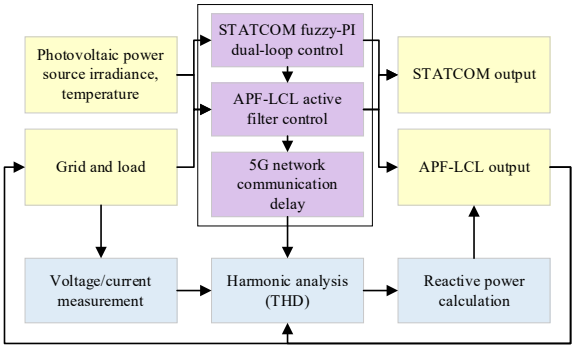

Figure 8: The Matlab/Simulink simulation architecture

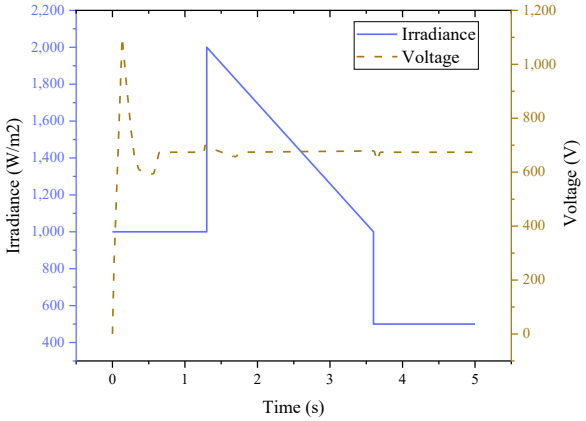

Figure 9: The influence of light intensity changes on DC bus voltage

In Figure 9, when the irradiance suddenly goes up from 1000 w/m^2 to 2000 w/m^2, the DC bus voltage quickly rises to 1100 v. When the irradiance drops sharply to 500 W/m^2, the voltage decreases to 754 V; meanwhile, it reaches a minimum of 594 V at 0.47 s. Subsequently, under the control of STATCOM and APF-LCL, the voltage gradually recovers to 674 V and stabilizes, and the fluctuation remains within 5%. The simulation demonstrates that the proposed compensation system exhibits strong dynamic response and voltage stabilization performance.

In the dynamic analysis of the system after connecting the reactive power compensation device, the voltage and current waveforms of the three-phase power supply are collected and plotted to visually demonstrate the improvement effect of the APF-LCL+STATCOM hybrid compensation system on the power quality of the grid connection point, as shown in Figure 10.

The figure shows the changes in three-phase voltage and corresponding three-phase current over time for A, B, and C.

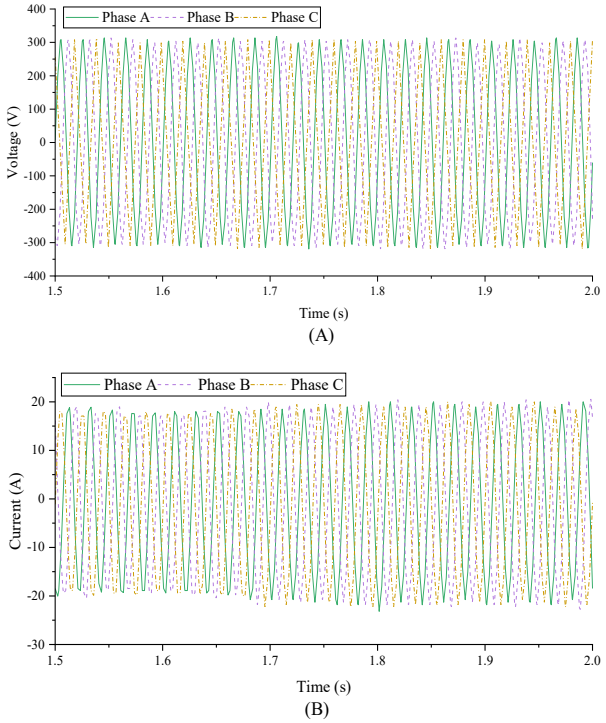

Figure 10: Three-phase power supply voltage and current waveform diagram after APF-LCL+STATCOM connection (A: the voltage waveform diagram, B: the current waveform diagram)

According to Figure 10, after the compensation device is connected, the waveform of the three-phase current tends to be sinusoidal, and the harmonic content is significantly reduced. The amplitude of the A, B, and C three-phase currents tends to balance, indicating that the APF-LCL module has good suppression ability for wideband harmonics. At the same time, the three-phase voltage waveform remains stable, and the peak voltage and fluctuation amplitude are controlled, demonstrating the effectiveness of STATCOM in dynamic reactive power support. Overall, this waveform validates the superior performance of the hybrid compensation system in improving current quality, suppressing harmonics, and enhancing system voltage stability, which meets the expected design goals.

Under constant lighting and temperature conditions, the STATCOM compensation device was connected at 1 second. The waveform of the photovoltaic grid connected current before and after the STATCOM was put into operation is shown in Figure 11.

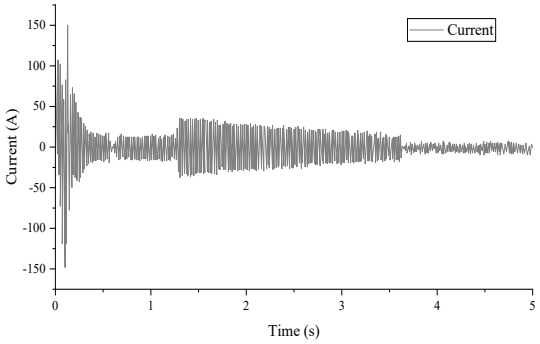

Figure 11: Photovoltaic grid connected current waveform before and after STATCOM input

As Figure 11 shows, the system current output is stable after connecting to STATCOM, with good waveform quality, stable amplitude, and no obvious distortion. Meanwhile, the current maintains a good phase relationship with the grid voltage, indicating that the inverter can achieve high-precision grid connected control under the fuzzy PI dual closed-loop control strategy. This result validates the dynamic reactive power compensation capability of STATCOM under this control strategy and the improvement effect on grid connected current stability.

To assess the harmonic mitigation performance of the STATCOM+APF-LCL system, a fast Fourier transform (FFT) analysis is performed on the grid current to extract and compare individual harmonic components and the total harmonic distortion (THD) before and after compensation. Assuming the fundamental current amplitude is 100%, harmonic components from the 3rd to the 15th order are selected as the analysis targets, and their amplitude variations under different compensation conditions are recorded. Figure 12 presents the harmonic spectrum of the grid current before and after compensation.

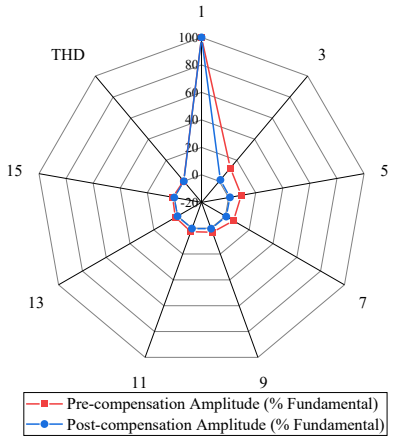

Figure 12: Harmonic spectrum of grid current before and after compensation

Figure 12 shows that the compensation system significantly reduces the amplitude of each harmonic component in the grid current, especially the 3rd, 5th, and 7th harmonics, which decrease from 12.6%, 9.4%, and 6.8% to 1.3%, 1.0%, and 0.7%, respectively. High-order harmonics are also effectively suppressed; the amplitude of the 11th order and above is reduced to below 0.3%. This shows that APF-LCL module provides effective wide-band harmonic filtering. THD is reduced from 17.30% to 2.60%; this significantly improves the power quality. The results confirm that the hybrid compensation system has good harmonic suppression performance and practical value.

4.3 Comparative Analysis of Different Control Strategies

In order to evaluate the superiority of the proposed control strategy, the double-loop, conventional PI and fuzzy-PI hybrid control strategy are compared and simulated. The comparison mainly focuses on three key performance aspects: reactive power compensation response time, harmonic suppression effect and system stability. Figure 13 illustrates the comparison results of these indicators.

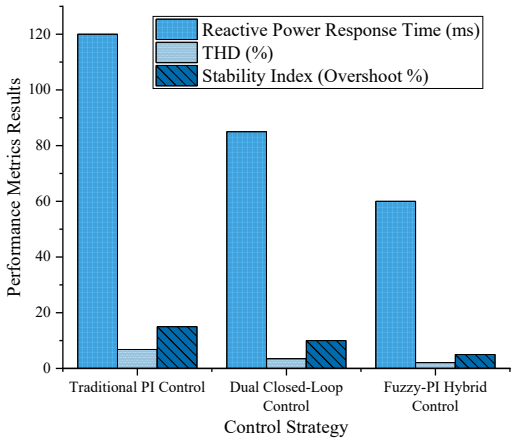

Figure 13: Performance comparison of different control strategies

In Figure 13, the fuzzy-PI hybrid control responds very quickly. It takes just 60 milliseconds (ms) to react. This is much better than the conventional PI control, which takes twice as long. It makes a big difference to how the system responds. Regarding harmonic suppression, the fuzzy-PI hybrid control reduces the THD to 2.1%; this is 69.1% and 40% lower than the THD levels of conventional PI control and dual-loop control. When it comes to system stability, the fuzzy-PI hybrid control has an overshoot rate of only 5%, lower than the other two strategies. This shows that it is more stable when there are load variations and external disturbances. Overall, the fuzzy-PI hybrid control strategy demonstrates the best performance in response speed, harmonic suppression, and system stability, making it well-suited for high-performance compensation requirements in the proposed system.

4.4 Simulation Analysis of Control Performance in 5G Network

A comparative simulation analysis is conducted on the effect of communication delay on the control closed loop's dynamic characteristics to verify the impact of 5G networks on the remote control performance of the STATCOM+APF-LCL hybrid compensation system under photovoltaic grid-connected conditions. In the simulation model, the communication network is equivalent to a fixed transport delay module in the control command transmission link. This delay directly acts on the current reference values and reactive power regulation commands sent from the main control center to edge control nodes; thus, it can reflect the impact of remote control on system dynamic response and stability under diverse communication conditions. Simulations are performed for comparison under two communication scenarios. (1) 5G network control mode. The main control center, edge nodes, and execution units communicate in real-time through a 5G network, assuming a delay of 10 ms and a packet loss rate of 0.1%. (2) Traditional Local Area Network (LAN) control mode. The same multi-level control architecture is used for communication through a regular local area network, assuming a delay of 50 ms and a packet loss rate of 1%. With the same control strategy and operating conditions, tests and comparisons are carried out on the system's current dynamic response (the time required for the actual output to reach 95% of the response value after a reference signal change), reactive power regulation accuracy, and voltage stability. Figure 14 presents the comparison results of the system current dynamic response under different communication conditions.

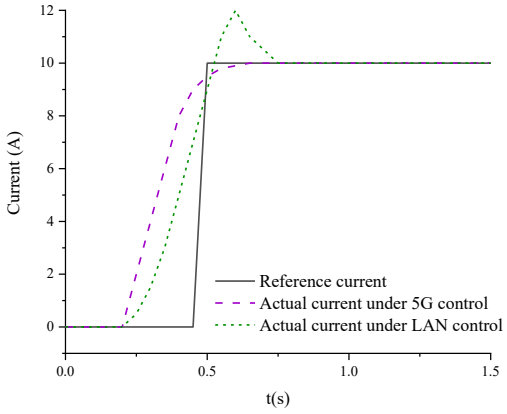

Figure 14: Comparison of the system current dynamic response under different communication conditions

In Figure 14, the reference current undergoes a step change at 0.5 seconds. Under the 5G network control mode, the system current can quickly track

the reference current command; meanwhile, it has a short response time, small fluctuation amplitude, and almost no obvious overshoot. This indicates that low-latency communication improves the real-time performance and stability of closed-loop control. In contrast, under the traditional LAN control mode, due to large communication delay, the current response shows obvious lag; the dynamic process presents large overshoot and requires a longer time to stabilize. This shows that communication delays can have a significant effect on how well the STATCOM+APF-LCL hybrid compensation system performs. When it comes to quantitative performance indicators, Table 2 compares system response performance under the two communication modes.

Table 2: Comparison of system response between traditional LAN and 5G network control modes

Control mode	Current response time (ms)	Reactive power regulation error (kVar)	Voltage fluctuation amplitude (V)
5G network control	12	0.8	2.1
Traditional LAN control	48	2.5	5.3

Table 2 suggests that in the 5G network control mode, the system response speed is remarkably improved; the current dynamic response is faster; besides, the response time is shortened by 75% compared to LAN control. The reactive power regulation error and voltage fluctuation amplitude have been reduced by 68% and 60.4%. This indicates that the low latency and high reliability of 5G networks can substantially enhance the real-time control performance and stability of the system. Under high-speed grid connection and dynamic load changes, 5G networks can ensure the rapid execution of control strategies and improve system power quality and robustness.

4.5 Sensitivity Analysis

To evaluate the designed STATCOM+APF-LCL hybrid compensation system's robustness under changes in key parameters, simulations are conducted on the system's response characteristics when the light intensity, load active power, and DC bus voltage reference value change. The main evaluation indicators include DC bus voltage fluctuation amplitude, current THD, and reactive power regulation error. The simulation results are outlined in Table 3.

Table 3: Sensitivity analysis results of the system under different parameter disturbances

Parameter perturbation type	Amplitude of variation	Bus voltage fluctuation range (V)	THD of current (%)	Reactive power error (kVar)
Light intensity	+20%	680–1120	2.8	1.1
Light intensity	-20%	630–1050	2.9	1.2
Load active power	+20%	660–1100	2.7	1.0
Load active power	-20%	640–1080	2.8	1.1
DC voltage reference	+10%	670–1110	2.6	1.0
DC voltage reference	-10%	650–1090	2.7	1.1

According to Table 3, when the light intensity, load active power and DC bus voltage reference value are subjected to disturbances of ±10% to ±20%. The DC bus voltage fluctuation range is maintained within a reasonable interval, without excessive overshoot or voltage sag. Meanwhile, the THD of grid current is kept within 3% under all operating conditions, and the reactive power regulation error is small with a variation range of no more than 1.5 kVar. This indicates that the designed STATCOM+APF-LCL hybrid compensation system has strong robustness against light changes, load fluctuations, and control target setting deviations. It can maintain stable voltage support and high-quality current output under diverse disturbance conditions; this ensures that the system power quality meets the design requirements.

This sensitivity analysis is based on the composite compensation structure and fuzzy-PI dual closed-loop control strategy proposed here, which is different from the analysis of traditional PI or single compensation devices in the literature. The results show that under multi parameter disturbance conditions, fuzzy PI control can dynamically adjust PI parameters to ensure stable system voltage support and current quality, highlighting the adaptability and innovation of the control scheme proposed here.

This provides a reliable design reference and verification basis for comprehensive power quality management in high proportion photovoltaic access scenarios.

4.6 Economic Analysis

In order to evaluate the advantages of the STATCOM+APF-LCL hybrid compensation system and 5G network control in operational efficiency and economy, a simulation analysis is performed on this system's active power loss, reactive power loss, and power factor under each control mode.

The annual operation economy is calculated based on the unit electricity price.

Table 4 illustrates the simulation results. The system operating conditions include photovoltaic grid connection, load active power of 10 kW, reactive power of 10 kVar, and constant light intensity and temperature.

Table 4: Comparison of system energy efficiency and economy under diverse control modes

Control mode/operating condition	Total system active power loss (kW)	Total system reactive power loss (kVar)	Power factor	Energy-saving effect (%)	Economic savings (CNY/year)
Without compensation	12.5	14	0.85	-	-
STATCOM+APF-LCL	10.2	1.5	0.98	18.4	5200
STATCOM+APF-LCL +5G network control	10.0	1.2	0.99	20	5700

It can be found from Table 4 that after connecting the STATCOM+APF-LCL hybrid compensation device, the system active power loss decreases by about 18%, the reactive power loss is significantly reduced, and the power factor is increased from 0.85 to 0.98. It achieves an obvious energy-saving effect and economic benefits. Further application of 5G network control accelerates the system response speed, further reduces losses, and the power factor reaches 0.99; annual electricity cost savings is about 5,700 yuan. The results show that the hybrid compensation device combined with high-speed communication control can improve power quality and it significantly enhances system operation efficiency and economy. Hence, it can provide a practical reference for the operation of distributed power sources under high-proportion photovoltaic grid-connected scenarios.

5. Conclusions

This study proposes a novel remotely controlled hybrid compensation system that integrates a STATCOM with an APF-LCL to provide coordinated reactive power compensation and harmonic suppression. A hierarchical control architecture based on 5G communication and edge computing is developed, incorporating an expert system and a fuzzy-PI dual-loop control strategy to achieve dynamic and coordinated compensation for reactive power and harmonics in PV grid-connected scenarios.

The simulation results show that under sudden changes in lighting conditions, the DC bus voltage fluctuation of the system is controlled within ±5%, and the three-phase grid connected current THD decreases from 17.3% before compensation to 2.6% after compensation. The amplitude of the key harmonic wave significantly decreases, and the reactive power fluctuation decreases from a maximum of 14kVar to 1.5kVar after compensation, with an average reduction of about 91%. Compared with traditional PI and dual closed-loop control, the fuzzy-PI control strategy shortens the reactive power response time to about 60 ms and controls the system overshoot rate within 5%. Under the conditions of a delay of 10 ms and a packet loss rate of 0.1%, the current response time of 5G network has been shortened from 48 ms of traditional LAN to 12 ms, the reactive power regulation error has been reduced from 2.5kVar to 0.8kVar, and the voltage fluctuation amplitude has been reduced from 5.3V to 2.1V, improving the real-time control and stability. In addition, preliminary economic analysis shows that the composite compensation system has certain advantages in energy consumption and operating costs, providing reference for engineering applications. Overall, this study validates the high-performance and multifunctional grid connected compensation capability of the proposed method under new energy access conditions, and provides numerical basis for dynamic compensation control strategies that meet the IEEE 519-2014 power quality standards.

However, there are still some limitations in this study. The model verification is mainly based on fixed temperature and light conditions; it does not cover more complicated climate, load disturbance and voltage fluctuation conditions. The performance of system robustness in multi-scenarios needs further evaluation. The rule base and fuzzy control parameter setting of expert system depend on

manual experience; its generalization ability is limited, so it may need to be optimized and adjusted based on real-time data in actual operation. In addition, there may be differences between simulation conditions and actual operating environments, so the conclusions drawn in this study still need further verification in practical engineering applications. In the future, the controller structure will be optimized by combining adaptive parameter adjustment mechanism and deep reinforcement learning; it can be extended to the hardware-in-the-loop experimental platform to improve the adaptability, real-time performance and engineering feasibility of the system in different power environments. On the whole, this study provides a method basis for the high-performance and multifunctional compensation system under the condition of new energy access; meanwhile, it preliminarily verifies the dynamic compensation control strategy that meets the power quality standards.

References

[1] Li B, Liu Z, Wu Y, et al. Review on photovoltaic with battery energy storage system for power supply to buildings: Challenges and opportunities. Journal of Energy Storage, 2023, 61, pp. 106763.

[2] Liang Y, Li P, Su W, et al. Development of green data center by configuring photovoltaic power generation and compressed air energy storage systems. Energy, 2024, 292, pp. 130516.

[3] G. Landera Y, C. Zevallos O, Neto R C, et al. A review of grid connection requirements for photovoltaic power plants. Energies, 2023, 16(5), pp. 2093.

[4] Behbahani M R, Jalilian A. Optimal operation of soft open point devices and distribution network reconfiguration in a harmonically polluted distribution network. Electric Power Systems Research, 2024, 237, pp. 110967.

[5] Gholami K, Azizivahed A, Arefi A, et al. Simultaneous allocation of soft open points and tie switches in harmonic polluted distribution networks. Electric power systems research, 2024, 234, pp. 110568.

[6] Rahimipour Behbahani M, Jalilian A. Reconfiguration of harmonic polluted distribution network using modified discrete particle swarm optimization equipped with smart radial method. IET Generation, Transmission & Distribution, 2023, 17(11), pp. 2563-2575.

[7] Tariq M B, Siddique A, Aslam W, et al. Tri-level Cascading Control to Augment Power Quality Concerns in Distribution Networks. Turkish Journal of Computer and Mathematics Education, 2024, 15(2), pp. 183-194.

[8] Stojanović B, Rajić T, Šošić D. Distribution network reconfiguration and reactive power compensation using a hybrid Simulated Annealing–Minimum spanning tree algorithm. International Journal of Electrical Power & Energy Systems, 2023, 147, pp. 108829.

[9] Xiang S, Xu D, Wang P, et al. Optimal expansion planning of 5G and distribution systems considering source-network-load-storage coordination. Applied Energy, 2024, 366, pp. 123372.

[10] Li X, Wang J, Lu Z, et al. A cloud edge computing method for economic dispatch of active distribution network with multi-microgrids. Electric Power Systems Research, 2023, 214, pp. 108806.

[11] Chuang X, Li L, Zhu L, et al. The design of a real-time monitoring and intelligent optimization data analysis framework for power plant production systems by 5G networks. Energy Informatics, 2025, 8(1), pp. 1-27.

[12] Fan P, Yang J, Ke S, et al. A multilayer voltage intelligent control strategy for distribution networks with v2g and power energy production-consumption units. International Journal of Electrical Power & Energy Systems, 2024, 159, pp. 110055.

[13] Guo W, Xu W. Research on optimization strategy of harmonic suppression and reactive power compensation of photovoltaic multifunctional grid connected inverter. International Journal of Electrical Power & Energy Systems, 2023, 145, pp. 108649.

[14] Bajaj M, Singh A K. A global power quality index for assessment in distributed energy systems connected to a harmonically polluted network. Energy Sources, Part A: Recovery, Utilization, and Environmental Effects, 2025, 47(1), pp. 8331-8357.

[15] Boopathi R, Indragandhi V. Enhancement of power quality in grid-connected systems using a predictive direct power controlled based PV-interfaced with multilevel inverter shunt active power filter. Scientific Reports, 2025, 15(1), pp. 7967.

[16] Kumar A, Mishra V M, Ranjan R. Fuzzy Distribution Static Compensator based control strategy to enhance low voltage ride through capability of hybrid renewable energy system. Energy Sources, Part A: Recovery, Utilization, and Environmental Effects, 2025, 47(1), pp. 8670-8687.

[17] Zheng Z A, Wei J C. Research on electric power steering fuzzy PI control strategy based on phase compensation. International Journal of Dynamics and Control, 2023, 11(4), pp. 1867-1879.

[18] Cheng Z, Wang L, Zeng S, et al. Partition-Global Dual-Layer Collaborative Voltage Control Strategy for Active Distribution Network with High Proportion of Renewable Energy. IEEE Access, 2024, 12, pp. 22546-22556.

[19] Ali Z M, Ćalasan M, Jurado F, et al. Complexities of power quality and harmonic-induced overheating in modern power grids studies: Challenges and solutions. IEEE Access, 2024, 12, pp. 151554-151597.

[20] Hamid A K, Mbungu N T, Elnady A, et al. A systematic review of grid-connected photovoltaic and photovoltaic/thermal systems: Benefits, challenges and mitigation. Energy & Environment, 2023, 34(7), pp. 2775-2814.

[21] Behbahani M R, Jalilian A, Bahmanyar A, et al. Comprehensive review on static and dynamic distribution network reconfiguration methodologies. Ieee Access, 2024, 12, pp. 9510-9525.

[22] Gao J H, Guo M F, Lin S, et al. Advancing high impedance fault localization via adaptive transient process calibration and multiscale correlation analysis in active distribution networks. Measurement, 2024, 229, pp. 114431.

[23] Dandea V, Grigoras G. Expert system integrating rule-based reasoning to voltage control in photovoltaic-systems-rich low voltage electric distribution networks: A review and results of a case study. Applied Sciences, 2023, 13(10), pp. 6158.